



# ANALYSIS OF ELECTRON TRANSPORT COEFFICIENTS IN GAS MIXTURES FOR PLASMA DISCHARGE IN ETCHING - SEMICONDUCTOR - A TREND IN MINING ELECTRICAL EQUIPMENT MANUFACTURING

Hien Xuan Pham<sup>1,\*</sup>, Tuoi Thi Phan<sup>2</sup>, Luong Vi Tran<sup>3</sup>, Hoa Ngoc Le<sup>4</sup>, Diep Thi Pham<sup>4</sup>

<sup>1</sup>University of Transport and Communications, 3 Cau Giay St., Ha Noi, Vietnam

<sup>2</sup>Hung Yen University of Technology and Education, Viet Tien C., Hung Yen, Vietnam

<sup>3</sup>Lai Chau Power Company, Dien Bien Phu Rd., Lai Chau, Vietnam

<sup>4</sup>Sao Do University, Chu Van An W., Hai Phong City, Vietnam

## ARTICLE INFOR

TYPE: Research Article

Received: 11/10/2025

Revised: 15/11/2025

Accepted: 18/11/2025

<sup>1,\*</sup> Corresponding author:

Email: hienpx@utc.edu.vn

## ABSTRACT

*This study presents the calculation and analysis of electron transport coefficients in gas mixtures composed of argon (Ar), molecular fluorine (F<sub>2</sub>), and nitrogen (N<sub>2</sub>), with a focus on their relevance to gas discharge applications. Using the BOLSIG+ Boltzmann solver and well-established electron collision cross-section data, key parameters such as mobility, diffusion coefficients, and ionization coefficients were evaluated across a range of reduced electric fields (E/N) and mixture ratios. These data serve as critical input for the modeling and optimization of low-temperature plasma discharges, particularly in applications such as reactive ion etching and thin film deposition using inductively coupled plasma systems.*

**Keywords:** Boltzmann equation, Ar–F<sub>2</sub>–N<sub>2</sub> gas mixtures, Plasma and Electron Discharges, mean electron energy

@ Vietnam Mining Science and Technology Association

## 1. INTRODUCTION

Modern microelectronics manufacturing has been significantly advanced by the planar process, which was pioneered by Jean Hoerni and his colleagues at Fairchild Semiconductor in the late 1950s [1]. Semiconductor fabrication involves a sequence of fundamental unit processes, including photolithography, plasma etching, wet chemical etching, thin film deposition, and Chemical Mechanical Polishing (CMP). Each of these steps plays a critical role in defining micro-scale structures and ensuring the quality and performance of the final semiconductor device.

Common techniques used in semiconductor manufacturing for material growth and deposition include thermal oxidation (used to grow silicon dioxide, SiO<sub>2</sub>, layers on silicon substrates),

Chemical Vapor Deposition (CVD), Physical Vapor Deposition (PVD), and Plasma-Enhanced Chemical Vapor Deposition (PECVD).

Thermal oxidation forms a high-quality silicon dioxide (SiO<sub>2</sub>) layer directly on the silicon wafer surface through a high-temperature chemical reaction in an oxidizing ambient. Chemical Vapor Deposition involves chemical reactions of gaseous precursors at elevated temperatures to deposit thin films with precise control over composition and uniformity. Physical Vapor Deposition is a physical process in which material is vaporized from a solid source in a vacuum environment and then condensed onto the substrate; common PVD techniques include sputtering and evaporation. Plasma-Enhanced Chemical Vapor Deposition utilizes plasma to activate chemical reactions at



lower temperatures, enabling the deposition of films such as silicon nitride or silicon oxide with excellent conformity and mechanical properties [2].

Film deposition represents a critical stage in semiconductor manufacturing, with CVD and PVD being the two main approaches for depositing thin films. In both techniques, the substrate is placed inside a deposition chamber, where the film-forming materials are delivered primarily in the gas phase to the substrate surface, resulting in thin film formation. For CVD, the film is formed through chemical reactions involving precursor gases on or near the substrate surface [1]. In PVD, physical processes generate atoms that travel through a low-pressure gas environment before condensing onto the substrate. A critical concern in all thin film deposition methods is the cleanliness of the deposition chamber. During the deposition process, the same materials that accumulate on the wafer also tend to deposit on the chamber walls [1].

Modeling plasma discharges is essential for understanding the complex dynamics and interactions between charged and neutral species within the plasma environment [3]. Effective modeling requires a comprehensive understanding of the various physical interactions between electrons and background gas molecules or atoms present in the plasma [4]. These physical phenomena include ionization, excitation, electron attachment, recombination, molecular dissociation, and elastic scattering events [5]. In recent years, molecular fluorine ( $F_2$ ) has attracted considerable attention in plasma etching applications within the semiconductor industry due to its zero global warming potential and superior etching selectivity compared to conventional gases [6].

Over the past few years,  $F_2$  has been widely utilized in plasma etching for semiconductor applications due to its zero global warming potential and excellent etching selectivity [7]. Fluorine is a pale yellow gas under standard atmospheric conditions [8]. Plasma processing using argon (Ar) is commonly employed in the fabrication of advanced semiconductor devices and high-efficiency solar cells [2]. Remote plasma etching of the SiOCH layer using an  $F_2$ /Ar mixture was performed by introducing  $N_2$  and/or  $O_2$  gases into the remote plasma source or by adding NO gas directly into the reactor. The chemical dry etching of the SiOCH layer was conducted by adjusting the flow ratios of  $F_2$ -Ar,  $N_2$ -Ar, and NO-Ar, as well as varying the etching temperature [9].

The selected Ar- $F_2$ - $N_2$  mixture possesses a zero global warming potential, rendering it environmentally friendly. This property supports

the semiconductor industry in meeting greenhouse gas emission reduction targets [10]. Due to its industrial significance and the necessity to investigate plasma phenomena, accurate electron transport coefficients and molecular cross-sections for these gases are essential [11]. Therefore, in this study, the electron transport coefficients—including mean energy, mobility, diffusion coefficient, and ionization coefficient of Ar- $F_2$ - $N_2$  mixtures were calculated and analyzed using the BOLSIG+ program [10]. The electron mobility characteristics of the Ar- $F_2$ - $N_2$  mixtures determined in this study can be exploited for the design of plasma systems for the fabrication of sensors and measuring devices in the mining environment. Plasma etching, plasma deposition or surface treatment processes can be used to produce gas-sensitive, thermosensitive materials or protective films resistant to harsh environments. Optimizing the Ar- $F_2$ - $N_2$  ratio and E/N conditions allows control of the ionization density and electron energy, thereby improving the uniformity of the sensitive film and the stability of the sensor. Target applications include gas sensors  $CH_4$ ,  $CO$ ,  $SO_2$ , pressure-temperature measuring devices in wellbore, and plasma probes used in mine safety warning systems [11].

## 2. MATERIALS AND METHOD

### 2.1. Theory

BOLSIG<sup>+</sup> software, developed by Hagelaar and Pitchford [12] in the mid-2000s, has been extensively utilized in low-temperature plasma physics and engineering research to calculate electron transport properties in gases and gas mixtures, such as electron mobility, mean energy, and diffusion coefficients. The mathematical framework underlying these calculations, including the solution of the Boltzmann equation using the two-term approximation and the derivation of the electron energy distribution function (EEDF), is comprehensively detailed in the original work by Hagelaar and Pitchford [12].

Briefly, the EEDF, denoted as  $f$ , is obtained by solving the Boltzmann equation under the two-term spherical harmonic expansion approximation, which separates the isotropic ( $f_0$ ) and anisotropic ( $f_1$ ) components of the distribution function. This approach provides the basis for calculating key electron transport parameters such as mean energy, mobility, and diffusion coefficients. For detailed mathematical expressions and derivations, the reader is referred to Hagelaar and Pitchford's original publication [12]. In this study,

these established formulations were employed directly within the BOLSIG<sup>+</sup> framework to compute the electron transport coefficients of Ar–F<sub>2</sub>–N<sub>2</sub> mixtures.

BOLSIG<sup>+</sup> widely used to calculate electron transport coefficients and has been successfully applied to various gases and their mixtures, including He and Ar [13], N<sub>2</sub> and SF<sub>6</sub> [14], as well as SiH<sub>4</sub> and C<sub>2</sub>H<sub>4</sub> [15]. A critical step in accurately determining electron transport coefficients is the selection of a reliable set of electron collision cross sections for the gas mixture under study. The cross sections for Ar atoms were obtained from established datasets determined by Kurachi and Nakamura [16], while those for F<sub>2</sub> molecules were provided by Jeon [17]. Electron collision cross section sets for N<sub>2</sub> atoms [18], as well as for Ar, F<sub>2</sub>, and N<sub>2</sub> molecules, are illustrated in Figures 1, 2, and 3, respectively.

Specifically, the electron collision cross section set for N<sub>2</sub> molecules, as determined by Nakamura, comprises one momentum-transfer cross section (C1), twenty vibrational excitation cross sections (C2–C24) with threshold energies ranging from 0.02 eV to 13 eV, and one ionization cross section Qi with a threshold energy of 15.6 eV. The cross section set for F<sub>2</sub> molecules includes one momentum transfer cross section, one attachment cross section (C1), eight electronic excitation cross sections (C3–C10) with threshold energies between 0.11 eV and 13.08 eV, and one total ionization cross section with a threshold energy of 15.69 eV. For Ar atoms, the collision cross section set consists of one momentum transfer cross section, one electronic excitation cross section, and one ionization cross section.

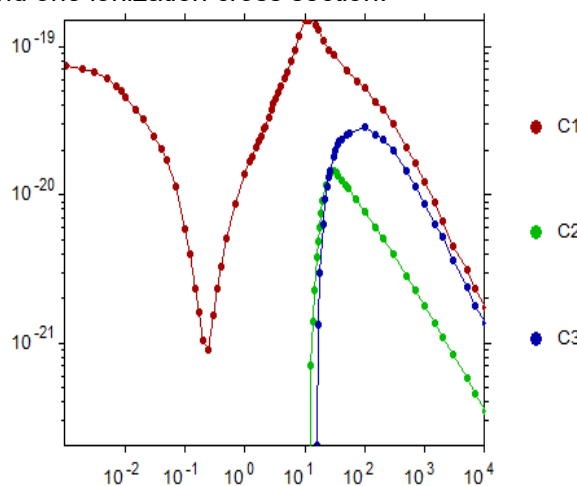


Figure 1. Dataset of electron collision cross sections for argon atoms

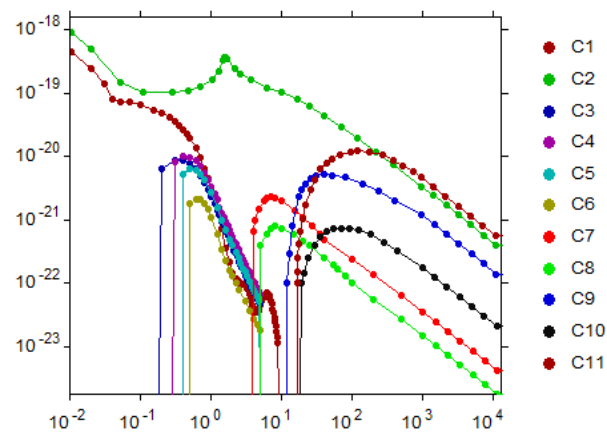


Figure 2. Dataset of electron collision cross sections for fluorine atoms

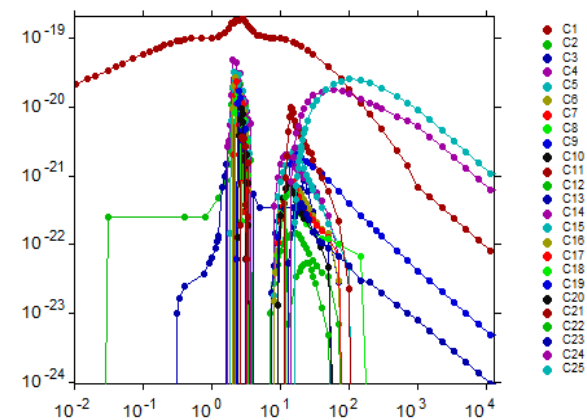
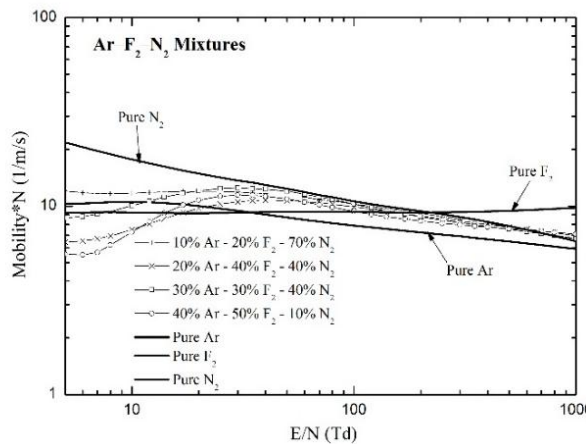


Figure 3. Dataset of electron collision cross sections for nitrogen atoms

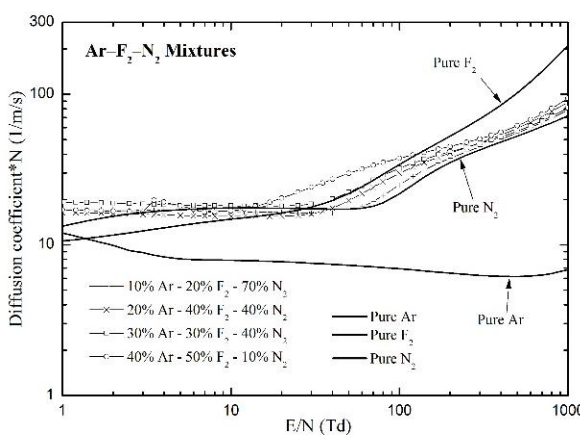
### 3. RESULTS AND DISCUSSION

Figure 4 presents the electron mobility ( $\mu^*N$ ) as a function of the reduced electric field (E/N) in various Ar–F<sub>2</sub>–N<sub>2</sub> gas mixtures over a range from 1 to 1000 Td. The mobility is shown in logarithmic scale, highlighting the transport behavior across mixtures with increasing concentrations of Ar, F<sub>2</sub>, and N<sub>2</sub>. The data indicate distinct trends for the pure gases: electron mobility decreases monotonically with increasing E/N in pure N<sub>2</sub> and F<sub>2</sub>, while pure Ar exhibits a slightly less steep decline. As E/N increases beyond 100 Td, the difference in mobility between various mixtures diminishes, indicating a potential convergence in electron energy distributions due to high-field effects.



**Figure 4. The mobility  $\mu^*N$  in the  $\text{Ar-F}_2\text{-N}_2$  mixtures**

Figure 5 shows the diffusion coefficient\* $N$  (DN) as a function of the reduced electric field (E/N) for various  $\text{Ar-F}_2\text{-N}_2$  gas mixtures, spanning the range from 1 to 1000 Td. The data are also plotted on a logarithmic scale to emphasize differences in diffusion behavior across mixtures with varying compositions. The pure gases exhibit markedly different characteristics: pure  $\text{N}_2$  shows a strong increase in DN with increasing E/N, indicative of significant energy gain and broader energy distribution at higher fields. Pure  $\text{F}_2$  also shows an increasing trend, though less steep, while pure Ar demonstrates a slight decrease followed by a gradual rise beyond 100 Td. The mixtures display intermediate diffusion behavior between the pure gases, with values increasing more slowly compared to pure  $\text{N}_2$ . As E/N exceeds 100 Td, the differences among the mixtures become more apparent, with  $\text{F}_2$ -rich mixtures diverging significantly from Ar-dominant ones.



**Figure 5. Diffusion coefficient\* $N$  in the  $\text{Ar-F}_2\text{-N}_2$  mixtures**

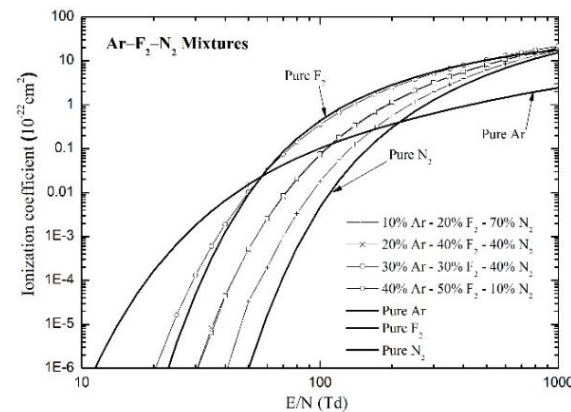


**Figure 6. Ionization coefficient in  $\text{Ar-F}_2\text{-N}_2$  mixtures**

Figure 6 presents the ionization coefficient ( $\alpha$ ) as a function of the reduced electric field (E/N) in various  $\text{Ar-F}_2\text{-N}_2$  mixtures, over a range from 10 to 1000 Td. The coefficient is plotted on a logarithmic scale to capture its strong exponential dependence on E/N.

Among the pure gases,  $\text{F}_2$  exhibits the highest ionization rate across all field strengths, followed by Ar, while  $\text{N}_2$  shows the lowest. Notably, the ionization in  $\text{F}_2$  begins to rise significantly at lower E/N values (30 Td), reflecting its higher efficiency in generating free electrons.

The mixtures demonstrate intermediate behavior, with ionization coefficients increasing more gradually than in pure  $\text{F}_2$ . Mixtures richer in Ar, such as the one with 40% Ar, 50%  $\text{F}_2$ , and 10%  $\text{N}_2$ , tend to show higher  $\alpha$  values at moderate to high E/N, due to the combined ionization contributions from both Ar and  $\text{F}_2$ . Conversely, mixtures with higher  $\text{N}_2$  content shift the onset of significant ionization to higher E/N, reducing the overall ionization rate.

When considered together with the results from Figures 4 and 5 (mobility and diffusion), the data in Figure 6 provide a complete perspective on electron behavior. Mixtures with high  $\text{F}_2$  content exhibit high ionization coefficients but lower mobility and diffusion, indicating dense electron production with limited transport. This trade-off is critical in designing gas systems for plasma discharges, where balancing ionization efficiency with electron transport is essential for stable operation.

#### 4. CONCLUSIONS

In this study, the electron transport parameters, namely the mobility, diffusion coefficient, and ionization coefficient, were systematically



calculated as functions of the reduced electric field ( $E/N$ ) for a range of Ar–F<sub>2</sub>–N<sub>2</sub> gas mixtures. These computations were carried out using the BOLSIG<sup>+</sup> solver, which relies on well-established electron collision cross-section data for argon (Ar), fluorine (F<sub>2</sub>), and nitrogen (N<sub>2</sub>). The resulting electron transport characteristics provide essential

reference data for modeling and simulation tasks in plasma physics. In particular, they are highly relevant for simulating inductively coupled plasma (ICP) processes involving Ar–F<sub>2</sub>–N<sub>2</sub> mixtures, which are widely applied in silicon etching technologies □

## REFERENCES

- [1]. An, J. (2008). Study of surface kinetics in PECVD chamber cleaning using remote plasma source. Doctoral dissertation, *Massachusetts Institute of Technology*. 163 pages.
- [2]. Plummer, J. D., Deal, M., & Griffin, P. B. (2000). *Silicon VLSI technology: Fundamentals, practice and modeling*. Prentice Hall, Upper Saddle River, NJ.
- [3]. Graves, D. B., Labelle, C. B., Kushner, M. J., Aydil, E. S., Donnelly, V. M., Chang, J. P., & others. (2024). Science challenges and research opportunities for plasma applications in microelectronics. *Journal of Vacuum Science & Technology B*, 42(4) 47 pages . DOI: 10.1116/6.0003531
- [4]. Parent, B., & Rodriguez Fuentes, F. M. (2024). Progress in electron energy modeling for plasma flows and discharges. *Physics of Fluids*, 36(8), 086113. DOI: 10.1063/5.0219552
- [5]. Benyoucef, D., & Yousfi, M. (2015). Particle modelling of magnetically confined oxygen plasma in low pressure radio frequency discharge. *Physics of Plasmas*, 22(1), 013510. DOI: <http://dx.doi.org/10.1063/1.4907178>
- [6]. De Wild-Scholten, M. J., Alsema, E. A., Fthenakis, V. M., Agostinelli, G., Dekkers, H., & Kinzig, V. (2007). *Title of the paper if available*. In *Proceedings of the 22nd European Photovoltaic Solar Energy Conference*, Milano, Italy.
- [7]. Tressaud, A. (2006). *Fluorine and the environment: Agrochemicals, archaeology, green chemistry and water (Vol. 2)*. Elsevier
- [8]. Cotton, F. A., Wilkinson, G., Murillo, C. A., & Bochmann, M. (1999). *Advanced inorganic chemistry* (6th ed.). Wiley-Interscience.
- [9]. Yun, Y. B., Park, S. M., Kim, D. J., Lee, N.-E., Choi, C. K., Kim, K. S., & Bae, G. H. (2008). Superior etch performance of Ar/N<sub>2</sub>/F<sub>2</sub> for PECVD chamber clean. *Thin Solid Films*, 516(12), 3549–3554.
- [10]. Benyoucef, D. (2024). Monte Carlo modeling and simulation of electron dynamics in low temperature methane gas. *Engineering, Technology & Applied Science Research*, 14(6), 18153–18159
- [11]. Zhou, J., et al (2022). “Advances in gas sensors for mining safety: Materials, structures, and challenges.” *Journal of Hazardous Materials*, 425.
- [12]. Hagelaar, G. J. M., & Pitchford, L. C. (2005). Solving the Boltzmann equation to obtain electron transport coefficients and rate coefficients for fluid models. *Plasma Sources Science and Technology*, 14, 722–733
- [13]. Ali, M. A., & Majeed, R. H. (2024). Calculation of electron transport parameters in noble gases: II. Helium and argon. *AIP Conference Proceedings*, 3097, 090012
- [14]. Ibrahim, S. I., Jawad, E. A., & Jassim, M. K. (2022). Study the effect of mixing N<sub>2</sub> with SF<sub>6</sub> gas on electron transport coefficients. *AIP Conference Proceedings*, 2386, 070003.
- [15]. Hien, P. X., Son, T. T., & Tuan, D. A. (2020). Studying electron transport coefficients in C<sub>2</sub>H<sub>4</sub>–SiH<sub>4</sub> mixtures using BOLSIG+ program. *Lecture Notes in Networks and Systems*, 178, 748–754.
- [16]. Nakamura, Y., & Kurachi, M. (1988). Electron transport parameters in argon and its momentum transfer cross section. *Journal of Physics D: Applied Physics*, 21(5), 718–722.
- [17]. Tuan, D. A., & Jeon, B.-H. (2011). Determination of the vibrational excitation cross-section for the F<sub>2</sub> molecule in a plasma discharge simulation. *Journal of the Korean Physical Society*, 58(4), 765–770
- [18]. Nakamura, Y. (2010). *Private communication*. Tokyo Denki University, Tokyo, Japan.



## PHÂN TÍCH CÁC HỆ SỐ CHUYỂN ĐỘNG ELECTRON TRONG HỖN HỢP ARGON–FLO–NITO CHO PHÓNG ĐIỆN PLASMA TRONG ỨNG DỤNG KHẮC BÁN DẪN - XU HƯỚNG TRONG CHẾ TẠO THIẾT BỊ ĐIỆN MỎ

Phạm Xuân Hiển<sup>1,\*</sup>, Phan Thị Tươi<sup>2</sup>, Trần Vi Lượng<sup>3</sup>, Lê Ngọc Hòa<sup>4</sup>, Phạm Thị Điện<sup>4</sup>

<sup>1</sup>Trường Đại Học Giao Thông Vận tải, 3 Cầu Giấy, Hà Nội, Việt Nam.

<sup>2</sup>Trường Đại Học Sư phạm Kỹ thuật Hưng Yên, Xã Việt Tiến, Hưng Yên, Việt Nam

<sup>3</sup> Công ty Điện lực Lai Châu, Đường Điện Biên Phủ, Lai Châu, Việt Nam

<sup>4</sup>Trường Đại học Sao Đỏ, Phường Chu Văn An, Tp. Hải Phòng, Việt Nam

### THÔNG TIN BÀI BÁO

CHUYÊN MỤC: Công trình khoa học

Ngày nhận bài: 11/10/2025

Ngày nhận bài sửa: 15/11/2025

Ngày chấp nhận đăng: 18/11/2025

Email: hienpx@utc.edu.vn

### TÓM TẮT

Nghiên cứu này trình bày các kết quả tính toán và phân tích các hệ số chuyển động của electron trong các hỗn hợp khí chứa argon (Ar), flo (F<sub>2</sub>) và nitơ (N<sub>2</sub>) để phục vụ cho các ứng dụng có phóng điện khí. Nghiên cứu sử dụng thuật toán giải phương trình Boltzmann và các bộ dữ liệu đã được xây dựng trong các nghiên cứu trước đó về tiết điện và chạm của các electron, các kết quả tính được bao gồm giá trị của các hệ số về độ động, khuếch tán và ion hóa trong một dải giá trị về điện trường E/N và tỷ lệ trộn trong hỗn hợp. Các dữ liệu tính toán được này là đầu vào quan trọng cho mô hình hóa và tối ưu hóa các phóng điện plasma nhiệt độ thấp, đặc biệt các ứng dụng như khắc ion phản ứng và lắng đọng màng mỏng sử dụng hệ thống plasma cảm ứng.

**Từ khóa:** phương trình Boltzmann, hỗn hợp khí Ar–F<sub>2</sub>–N<sub>2</sub>, phóng điện plasma, năng lượng trung bình của electron

@ Hội Khoa học và Công nghệ Mỏ Việt Nam